Fluorescence lifetime imaging microscopy (FLIM) analysis of defects in multi-tube physical vapour transport grown $Cd_{1-x}Zn_xTe$

Andreas Schneider, Matthew C Veale, Steve J Bell, Diana D Duarte, Matthew D Wilson, Paul Seller, Stanley W Botchway, Ashutosh Choubey and Douglas Halliday

Published version information

This is the peer reviewed version of the following article:

Citation: Schneider, A et al. "Fluorescence lifetime imaging microscopy analysis of defects in multi-tube physical vapor transport grown $Cd_{1-x}Zn_xTe$." Physica Status Solidi A, vol. 211, no. 9 (2014): 2121-2125.

which has been published in final form at 10.1002/pssa.201300724. This article may be used for non-commercial purposes in accordance With Wiley-VCH Terms and Conditions for self-archiving.

Please cite only the published version using the reference above.

Phys. Status Solidi A, 1–5 (2014) / DOI 10.1002/pssa.201300724 (author's manuscript)

Fluorescence Lifetime Imaging Microscopy (FLIM) analysis of defects in Multi-Tube Physical Vapour Transport grown $Cd_{1-x}Zn_xTe$

Andreas Schneider[*,1], Matthew C Veale[1], Steve J Bell[2], Diana D Duarte[1,2], Matthew D Wilson[1], Paul Seller[1], Stanley W Botchway[1], Ashutosh Choubey[3] and Douglas Halliday[3]

[1] Science and Technology Facility Council - Rutherford Appleton Laboratory, Detector Development Group & Central Laser Facility, Harwell Oxford, Didcot, OX11 0QX, United Kingdom
[2] Faculty of Engineering and Physical Sciences, University of Surrey, Guildford, Surrey, GU2 7XH, United Kingdom
[3] Department of Physics, Durham University, Rochester Building, South Road, Durham, DH1 3LE, United Kingdom

Received 30 October 2013, revised ZZZ, accepted 11 March 2014
Published online 11 March 2014 (Dates will be provided by the publisher.)

Keywords FLIM, CZT, fluorescence lifetime, crystalline defects.

* Corresponding author: andreas.schneider@stfc.ac.uk, Phone: +44 1235 44 6164

Cadmium zinc telluride (CZT) is the material of choice for high-energy room-temperature X-ray and γ-ray detectors. However, the performance of pixelated detectors is greatly influenced by the quality of CZT. Crystal defects and impurities are one source of shallow and deep level traps for charge carriers. Fluorescence lifetime of the recombination of optically excited charges may indicate the presence and type of defects and impurities in CZT. Fluorescence Lifetime Imaging Microscopy (FLIM) is used to examine the excited-state lifetime in CZT fabricated by different growth methods and conditions. The FLIM set-up analyses luminescence emitted from the sample following photo excitation. Samples were optically excited above band gap with a pulsed laser (590 nm) for raster scanning a 220µm×165µm sample area. In-situ room-temperature photoluminescence (PL) and FLIM were recorded simultaneously. In order to analyse the FLIM data, two dominant charge carrier decay processes (τ_1, τ_2) were identified. The luminescence signal decays with a rapid lifetime of $\tau_1 \approx$ 50ps to 200ps, and a large variety of long-lifetime components τ_2 were found in the range of 225ps to 900ps. CZT grown by Multi-Tube Physical Vapour Transport (MTPVT) showed extremely long-lived recombination decay times up to 3.5ns in the vicinity of the interface at growth start. Further away from this interface, the recombination lifetime was in the typical range of fast transitions similar to those found in detector-grade CZT fabricated by Travelling Heater Method. Crystalline material quality strongly influences FLIM lifetime.

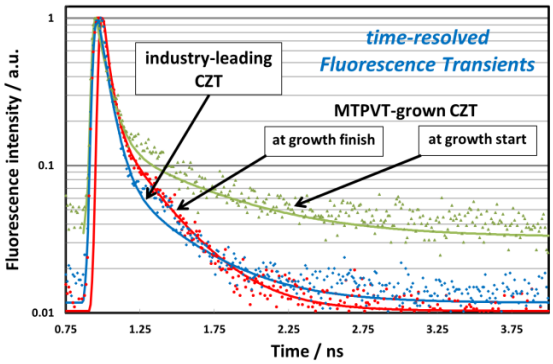

Abstract Figure Time-resolved transients of MTPVT-grown CZT compared with industry-leading detector grade CZT (dots: measured data; lines: fitted exponential decay curves).

1 Introduction High-energy X-ray / γ-ray spectroscopy is often used in applications for materials science and medical imaging. It requires detectors that have high efficiency at energies >30 keV. Spectroscopic detectors produced in Si do not have sufficient stopping power at these energies and Ge detectors require cryogenic cooling. Cadmium Telluride (CdTe) and Cd-rich ternary tellurides are better suited materials as they operate at room temperature

and have excellent spectroscopic energy resolution of 0.8keV measured at 60keV [1]. Despite this excellent performance, CdTe detectors are limited to 1mm thickness due to large leakage currents at typical operating voltages >500V. $Cd_{1-x}Zn_xTe$ (CZT) alloys with a Zn fraction of typical x~0.1 have a larger band gap and a higher resistivity than CdTe which reduces leakage currents and permits thicker (>1mm) detectors. Still, the growth of large quantities of good quality mono-crystalline CZT is a challenge.

Fluorescence Lifetime Imaging Microscopy (FLIM) was used to characterise the crystalline quality of CZT. FLIM is a time-resolved optical characterization method, which examines the decay of the entirely emitted fluorescence from a sample under excitation of a pulsed laser in order to determine the recombination lifetime of excited states. Generally FLIM is used for analysing fluorescent molecules in chemical and biological applications [2] but it also allows recombination pathways of photo-generated charge carriers in semiconductors to be examined. Several groups have used picosecond time-resolved luminescence measurements in CdTe and (Cd,Mn)Te [3-5]. In this work, we use FLIM to scan CZT for the first time and to map its lifetime distribution of transitions. We aim to investigate the excited-state lifetime of charge carriers and their recombination processes, particularly those involving trap states which influence the electronic properties of CZT.

2 Experimental setup

2.1 Material This study focuses on material grown by Multi-Tube Physical Vapour Transport (MTPVT). MTPVT is controlled by the mass flow of the evaporation of binary compounds CdTe and ZnTe. The ternary CZT can be grown from vapour at a comparatively low growth temperature, thus avoiding a melt phase of CZT, reducing impurities and minimizing the generation of Te inclusions [6]. For our investigation, a CZT boule (2-inch diameter, 20mm thick) was grown. The growth process consisted of an initial CdTe nucleation layer of a few millimetres grown on a GaAs (111) substrate followed by the growth of CZT at 740°C with a growth rate of ~360µm/h and a ~9.5% Zn content estimated by weight. A resistivity up to $2.3\times10^{11}\Omega$cm was measured for a crystal specimen cut out of the boule indicating its potential use as an X-ray detector material. Further details on growth and crystal characterization of the MTPVT-CZT are reported elsewhere [6]. For the FLIM and PL analysis of MTPVT-CZT, different parts of an as-grown boule were used. The boule was sliced into wafers (3mm thick) perpendicular to the direction of growth using a wire saw (AWS Logitech) and silicon carbide slurry. The cutting surfaces were subsequently lapped and polished with a Logitech PM5 polishing system using Al_2O_3 slurry with grain size down to 0.3µm. Three wafers of the boule were investigated: one from the tip (A), one between tip and heel (B), and one at the heel in the vicinity of CdTe buffer/CZT growth start (C). Commercially available detector-grade indium-doped CZT crystal (CZT:In), fabricated by Redlen Technology using Traveling Heater Method (THM), was used as reference in comparison to the MTPVT material. Redlen material is known to produce X-ray detectors with excellent spectroscopic resolution [7].

2.2 FLIM and PL FLIM experiments were carried out with samples described in 2.1 using optical excitation of CZT above their band gap energy. An optical parametric oscillator (590nm) pumped by a pulsed 76MHz, 180fs Titanium sapphire (Ti:Sapph) laser was used for mapping 220µm×165µm crystal areas with a laser focus size of ~0.5µm. A Hamamatsu R3809U MCP photomultiplier tube, sensitive from 300nm to 850nm, was used to record the decay transients of each excited spot. In-situ room-temperature PL and FLIM were recorded simultaneously. For PL at room temperature (RT), an Acton 275 spectrometer with an attached Andor CCD camera (iDus DU420) was used.

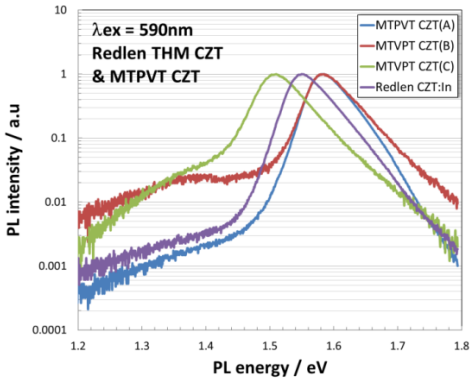

Figure 1 RT PL of CZT:In and three MTPVT-CZT samples which were cut from different positions (A,B,C) of the boule.

3 Results

3.1 Room-temperature (RT) PL Fig.1 relates the RT PL spectra of Redlen CZT:In and the various cuts of the MTPVT-CZT. All spectra are normalized to the PL maximum for better comparison. Spectra of all samples are broad due to the typical thermal broadening but exhibit distinctive maxima that are correlated to the near band edge emission and hence to the Zn-content of each sample.

The spectrum (green) of the MTPVT-CZT at position C close to the growth start shows the lowest PL maximum. The Zn content in sample C is negligible, according to calculations using the empirical formula, which describes the relation of RT PL and the zinc fraction in CZT [8]. This part of the sample represents largely the CdTe nucleation layer. This spectrum has a considerable PL in the range below 1.45eV (deep level donor–acceptor transitions at mid-band gap) indicating a significant number of defects in the CdTe layer at the growth start of CZT. The lattice mismatch between the CdTe buffer layer and the GaAs(111) substrate can lead to the introduction of crystalline defects, which are often associated with deep level complexes in

the band gap [9]. The maximum of the spectrum taken from the MTPVT-CZT at position B between heel and tip of the boule, where CZT growth has already taken place, is shifted to a higher energy and is correlated to a Zn content of x~0.12. A considerable amount of PL is still visible in the energy range below 1.45eV. For both samples, B and C, the near band edge PL is only 50-times larger than the emission from these deeper levels. This indicates that a significant number of crystalline defects still exist in position B. Only at the tip of the boule (A), has the amount of PL in the range below 1.45eV decreased; the ratio between PL maximum and the PL contribution from mid-band gap states below 1.45eV is comparable to the ratio which was observed in the CZT:In sample. The ratio between near band edge PL and deep level PL is ~400:1 and ~625:1 for CZT(A) and CZT:In, respectively. This indicates that after the MTPVT growth of CZT for several hours – until a crystal has a length of >6mm – the crystalline quality starts to improve and is comparable to the quality of Redlen's detector grade CZT:In. The spectrum of the CZT:In has a PL maximum at about 1.55eV which represents a Zn content of x~0.07.

3.2 FLIM data analysis In order to analyse the time-resolved recombination of photo-generated charge carriers created by the pulsed laser, the luminescence decay signal of each transient was fitted to an exponential decay function using SPCImage data analysis software. The exponential decay function $f(t)$ expresses the decease of luminescence with time t caused by a number N of possible recombination processes i:

$$f(t) = \sum_{i=1}^{N} a_i \exp(-t/\tau_i) \quad (1)$$

Typical recombination processes of the excited charge carriers in CZT are band-to-band, donor–acceptor recombination, and transitions from deep level traps within the band gap, each of which has a typical lifetime τ_i. The factor a_i indicates the percentage contribution to the total luminescence. A good fit to transient data was achieved by using the exponential decay of two principal recombination processes (τ_1: fast decay, τ_2: slow decay) on condition that the reduced chi-square χ^2 is close to unity as a test of accuracy. Typical transients (data and fit curves) are shown in the Abstract Figure. The industry-leading CZT from Redlen and the MTPVT-grown CZT of the samples as described in 2.1 and 3.1 are compared in terms of excited-state lifetime. For better visualisation, all transients in the Abstract Figure were normalized to each signal maximum at excitation. Data points of the MTPVT-CZT sample from the boule tip (position A at growth finish) follow almost the same time progression as for the Redlen material, hence the similar time constants. The time constant τ_1 for the fast process is close to the FLIM system response time, 50ps, but the lifetime of the long-lived process is τ_2~295ps. At first, the MTPVT-CZT (C) signal curve is similar to that of the two other samples, then the signal decay slows down indicating different slow recombination processes here (τ_1~79ps; τ_2~580ps). All fit curves are significant approximations to the data with χ^2=1.19, 1.47, and 1.1 for CZT:In, MTPVT-CZT (A), and MTPVT-CZT (C), respectively.

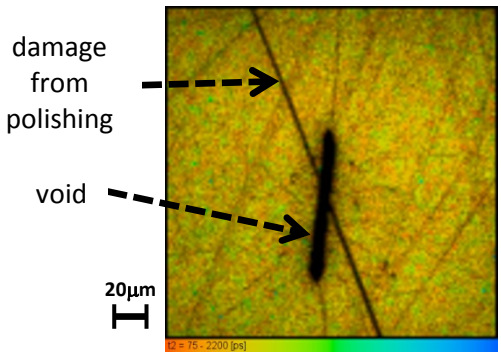

Figure 2 FLIM map of lifetime τ_2 (slow process) in an MTPVT-grown CZT crystal at the tip of the boule (position A).

3.3 FLIM mapping of MTPVT-CZT and CZT:In For a closer analysis, these three samples were mapped by the laser specified in 2.2. As described in 3.2, the decay data from each excited pixel were analysed and maps for the fast (τ_1) and the slow (τ_2) recombination lifetime were generated. These maps can be used to correlate crystal defects to a particular lifetime. Voids are the most prevalent defects in MTPVT material. The crystals also tend to have grain boundaries and dislocations [6]. These defects have an influence on the lifetime of the excited charge carriers.

Fig.2 and Fig.3 are examples of FLIM maps. An identical colour code was chosen for the range of lifetime (75ps <τ_2< 2200ps); bright red indicates short lifetime and dark blue long lifetime. Due to the sensitivity of the FLIM detector, these maps take only the luminescence above ~1.459 eV into account, which covers the PL maxima in Fig. 1. Fig.2 is a map across an area of MTPVT sample A, which has several defects such as scratches and a large void extending over several µm. These defects were revealed after the lapping/polishing process. Despite these obvious defects along which defect states were expected, homogeneous recombination properties across the sampled area were observed. Although Fig.2 maps the longer time constant τ_2 in formula (1), these charge carrier states are relatively short-lived with a lifetime as fast as 225ps but not exceeding 900ps.

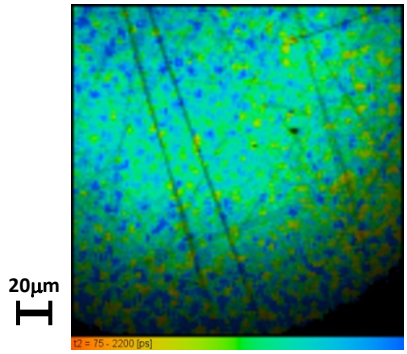

Figure 3 FLIM map of lifetime τ_2 in an MTPVT-grown CZT crystal at growth start (position C).

Using an excitation (590nm) above the band gap, laser light penetrates only a few nm into CZT and hence transitions are dominated by surface defect states instead of extended defects such as voids. The MTPVT sample C has a similar homogeneous and random lifetime distribution with no particular pattern (Fig. 3) but most transitions were far more long-lived than those in sample A, typically >1ns. The distribution of the lifetime mapped across MTPVT samples A and C was plotted for τ_1 and τ_2 in Fig.4(a+b) in comparison with CZT:In. Fig. 4 shows that the lifetime for both the fast and slow decay in Redlen CZT:In exists in a narrow interval centred around τ_1~87ps and τ_2~370ps. For the MTPVT-CZT samples, the lifetime intervals are much broader and the lifetime maxima are shifted relative to the extrema for CZT:In. At the tip of the MTPVT-CZT (A) the fast recombinations occur at shorter time (~80ps) but vary from 50ps to 200ps. At the same sample position (A), the slow recombination transients have a lifetime $225\text{ps} < \tau_2 < 900\text{ps}$ with most transitions at 500ps. This marginal difference between the two samples can possibly be attributed to the fact that MTPVT-CTZ (A) is not compensated by In-dopants and hence this allows a larger number of different optical recombination processes to occur. The similarity in lifetime between those two samples illustrates that MTPVT-CZT is potential detector-grade material. In contrast, the lifetime of recombinations near the heel of the MTPVT-CZT boule (position C) is shifted to far longer recombination processes and has a much broader distribution with some transitions as fast as 50ps for τ_1 but the majority of short-lived excited states with a decay time between 100ps to 300ps (maximum at 180ps). For slow transitions, a significant number between 500ps and 2500ps with a maximum at τ_2~1420ps and a few long-lived recombinations up to 3.5ns were observed. This drastic change of the lifetime characteristic demonstrates poor crystalline quality at the interface between CdTe buffer layer and growth start of CZT. Defects such as dislocations, impurities, change in Zn content, and stress caused by lattice mismatch between CdTe and CZT can be the source of various long-lived transition pathways. Some of them may be associated with trap-assisted processes. A similar influence on the lifetime of photo-generated charges has also been observed by other groups [4,5]. Long-lived transitions increase from 1.82ns up to 73ns by annealing CdTe [4] and doping of (Cd,Mn)Te increases the transient lifetime from 60ps to 960ps [5]. However, doping of CZT seems to have only a minor influence on the transient lifetime.

4 Conclusion FLIM mapping of CZT has been demonstrated as a complementary tool for the characterization of CZT. The recombination of excited charge carries in CZT can be described by two dominant lifetime components, one fast component τ_1 and a slow one τ_2. For detector-grade CZT:In these are typically τ_1~87ps and τ_2>200ps with a maximum at 370ps. MTPVT-grown CZT showed similar transitions but a broader lifetime distribution at the tip of the boule and is still considered as potential detector-grade material. In contrast, the same sample showed far longer lifetime in the first 6mm of the boule with up to 3.5ns (maximum τ_1~180ps and τ_2~1420ps). This is attributed to poor crystalline quality at the interface to the growth start and can be associated with trap states. RT PL corroborates these results.

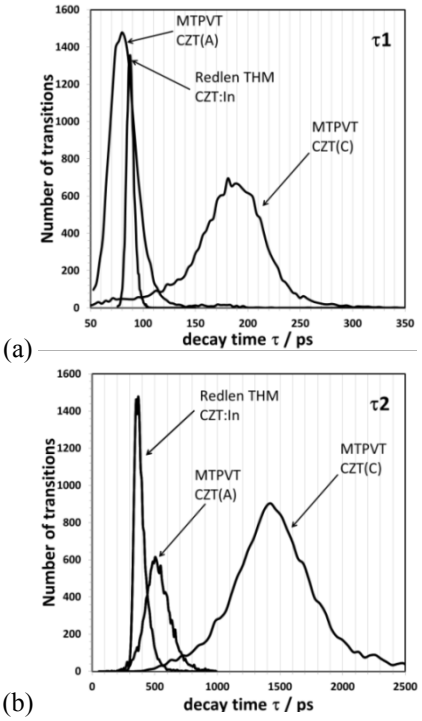

Figure 4 Number of transitions for fast (a) and slow recombinations (b) in typical Redlen CZT:In and in MTPVT-CZT (A & C).

Acknowledgements We would like to thank Redlen Technologies for samples and the Research Complex at Harwell (UK) for access to the FLIM system. This work was funded by EPSRC Basic Technology Grant - HEXITEC and by STFC.

References

[1] M. C. Veale, J. Kalliopuska, H. Pohjonen, et al., JINST **7**, C01035 (2012).

[2] R. H. Bisby, S. W. Botchway, J. A. Hadfield, et al., Eur. J. Cancer **48**, 1896-1903 (2012).
[3] G. Ghislotti, D. Ielmini, E. Riedo, M. Martinelli, and M. Dellagiovanna, Solid State Commun. **111**, 211-216 (1999)
[4] E.S. Barnard, E.T. Hoke, S.T. Connor, et al., Nature - Scientific reports **3**, Article number 2098 (2013).
[5] A. Mycielski, personal communication at E-MRS fall meeting, Symposium N (2013).
[6] A. Choubey, P Veeramani, A.T.G. Pym, J.T. Mullins, et al., J. Crystal Growth **352**, 120-123 (2012).
[7] H.Chen, S. A. Awadalla, F. Harris, et al., IEEE Trans. Nucl. Sci. **55**, 1567-1572 (2008)
[8] S.P.Tobin, J.P. Tower, P.W. Norton, D. Chandler-Horowitz, et al., J. Electron. Mater. **24**, 697-705 (1995).
[9] T.E. Schlesinger, J.E. Toney, H. Yoon, E.Y. Lee, et al., Mater. Sci Eng. **32**, 103-189 (2001)